ISSN 1070-4272, Russian Journal of Applied Chemistry, 2019, Vol. 92, No. 7, pp. 933−939. © Pleiades Publishing, Ltd., 2019.

CATALYSIS

Ethylene to Propylene over Zeolite ZSM-5: Improved Catalyst Performance by Treatment with CuO

Ehsan Kianfar[a,b,*]

[a] *Department of Chemical Engineering, Arak Branch, Islamic Azad University, Arak, Iran*
[b] *Young Researchers and Elite Club, Gachsaran Branch, Islamic Azad University, Gachsaran, Iran*
**e-mail: e-kianfar94@iau-arak.ac.ir*

Received January 30, 2019; revised May 20, 2019; accepted June 26, 2019

Abstract—In this paper, the ZSM-5 zeolite base is used to produce light olefins in the process of converting ethylene to propylene, as well as copper oxide to improve the catalyst. After loading the copper oxide by inoculation, the modified catalyst was investigated for accurate determination of the specification by XRD, SEM, BET, and FTIR analyzes. The activity of this catalyst was evaluated in the process of ethylene to propylene conversion in a constant reactor under operational conditions (temperature 400°C, pressure 1 atm, and feed flow rate of 0.5 cc min^{-1} of pure ethylene), which also shows the results of tests of catalyst activity evaluation The modified catalyst of selectivity of ethylene and propylene will increase as the temperature rises and the maximum selectivity table at 400°C will be achieved.

Keywords: ethylene to propylene process, fixed-bed reactor, ZSM-5 catalyst

DOI: 10.1134/S1070427219070085

INTRODUCTION

Since the synthetic drugs are not easily absorbed by human body and have certain toxic and side effect, people prefer to extract the medicinal ingredients from plants. Flavonoids are a kind of natural substances which are widely present in plants and have important medicinal values. In recent years, the study of flavonoids has been inclined to focus on the applied study of extraction and separation process. The method of extracting quercetin, one of the main constituents of flavonoids, is also being studied and improved [1, 2]. At present, the main extraction methods are: organic solvent extraction, ultrasonic extraction, enzyme extraction, supercritical fluid extraction, macroporous resin adsorbing method and so on, but all of them are flawed by cumbersome process, high equipment cost, poor purity and other problems to some extent [3].

The application of molecularly imprinted solid phase extraction (MISPE) in the separation and purification of the effective constituents in plant samples has not only retain the advantages of simple operation and low solvent dosage of solid phase extraction, but also acquire the excellent property of specific recognition of molecularly imprinted polymers [4–6]. Presently, some research groups have studied the preparations and applications of quercetin molecularly imprinted polymers [7–9]. Pakade et al. [10] have synthesized MIP with the bulk polymerization method using quercetin as template molecule, and established the MISPE method to enrich and separate the quercetin in horseradish tree leaf, flower, kaempferol and other flavonoids. The recovery result was good and the recovery rate was 75–86%.

Reversible addition-fragmentation chain transfer free radical polymerization (RAFT) is a widely used active/controllable free radical technology, which can control the structure and property of polymers [11, 12]. Reversible addition-fragmentation chain transfer free radical polymerization combined with precipitation polymerization method (RAFTPP), through the control of reaction speed, is able to obtain the imprinted microsphere with a uniform particle size and good dispersity, so that it can be more widely used [13, 14]. The aim of this paper is to use RAFTPP method to prepare quercetin molecularly

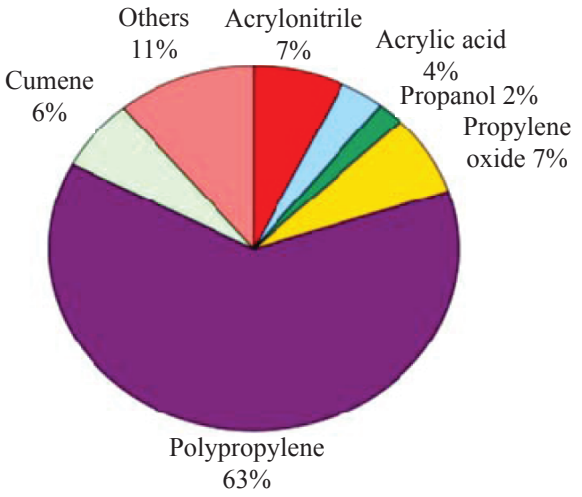

Fig. 1. (Color online) Products of propylene [5].

INTRODUCTION

Light olefins (ethylene and propylene), are considered among the most crucial elements in petrochemical industries, which are used for producing polymers and diverse chemicals. As the main feed of petrochemical processes, propylene is widely used [1–3]. Figure 1 shows the percentage of using propylene for each production: 63% is used for polypropylene, 7% is used for acrylonitrile, 7% is used for propylene oxide, 6% is used for cumene, 4% is used for acrylic acid, 2% is used for isopropanol and 11% used for production of other chemicals [4, 5]. Olefins can be produced through diverse processes and different raw materials. The common point of all these processes is production in a wide range of products and production of peripherals. In addition to mentioned industrial processes, there exist additional non-industrial technologies in diverse development steps including oxidative coupling of methane (OCM), propane dehydrogenation (PDH) for production of propylene, low-value heavy olefins cracking exemplary C4/C5, metathesis of ethylene and butylene to propylene and conversion of methanol to light olefins (MTP, MTO) [6–10]. Concerning access to hydrocarbon resources in different countries, diverse strategies are selected for production of olefins so that upon discovery of such strategies, propylene to ethylene ratio has been considerably decreased in steam cracking units and this has resulted in complicated propylene market [11–14]. Although Thermal Cracking of Naphtha is the main process of light olefins production such as propylene, such technologies as Fluid Catalytic Cracking (FCC) and Thermal Cracking of Ethan are classified as the methods with low efficiency [15–20]. The steam cracking process is implemented in a temperature of about 800–880°C and nearly 40% of energy is consumed by all of the petrochemical industries with high emissions of CO_2, what the development of advanced techniques not only results in minimized energy consumption but also decreases emissions of CO_2. This concern can be important to protect the environment [20–25]. In addition, according to limited P/E (propylene to ethylene) ration control in steam cracking process where olefins are directly depended on the feed type and also the higher growth of global demand for propylene compared to ethylene [26, 27]. Studies indicate that, according to increase demand for propylene in the global market, it makes sense to find alternative methods for propylene production. [28]. It is well understood that low numbers of Brønsted acid sites leads to higher selectivity to light olefins in conversion of methanol to hydrocarbons . Observed that an increase in Si/Al in the ZSM-5 zeolite framework leads to a pronounced decrease in total acidity of the zeolite and consequently in acidic site density. Studied the effect of acidity on product selectivity in conversion of methanol to hydrocarbon, by changing the SiO_2/Al_2O_3 ratio from 35 to 1670 in ZSM-5 zeolite. They observed that by increasing this ratio, the selectivity to C2/C5 olefins is increased. [22]. Zeolites as catalysts have many unique properties such as acidity, shape-selectivity, high surface area and structural stability. The destination of this article is using the ZSM-5 catalytic process for producing light olefins. This works destination is synthesized and specify characteristics of CuO/ZSM-5 study and assess the role of this catalyst in ethylene to propylene process. In doing so, direct conversion of ethylene to propylene may be an efficient way to be responsive global demand. Here, ethylene was used as a feed. Also, insemination of modified zeolite by CuO caused to reach a propylene with higher conversion rate and selectivity. The catalyst with 5 wt. % copper oxide has the highest conversion rate and better selectivity than other percentages.

MATERIALS AND METHODS

Materials

Sodium aluminate (technical grade) was purchased Riedel-deHaen. Silicic acid (96.6%), tetrapropylammonium bromide (98%), copper (II) nitrate (99.9%),

sodium hydroxide (97.5%), methanol (99.9%), ethanol (96%), ammonium nitrate (99.95%) was supplied by Merck.

METHOD AND PROCEDURE

Zeolite ZSM-5 Catalyst Synthesis

Initially the desired amount of sodium aluminate was added to hydroxide sodium solution and stirred for 60 min (solution A). In another beaker, required amount of tetra-propyl-ammonium bromide was added to sodium hydroxide solution and stirred for 30 min. Silicic acid and deionised water were slowly added and stirred for another 30 min (solution B). Subsequently, solution A was mixed with solution B and stirred for 60 min. Final gel was transferred to a Teflon-lined stainless steel autoclave and heated at 180°C for 12 h. Finally, contents of reactor were filtered, washed and dried at temperature 110°C for 12 h. The solid product was calcined at 500°C for 5 h. Ion exchanging of ZSM-5 zeolite performed using ammonium nitrate solution (1 M). Zeolite was mixed with solution and heated at 110°C for 6 h. In following step, silica foam was added to the solution while mixing. After 24 h of mixing, the derived gel was poured into an autoclave reactor and heated at 150°C for 6 days. Catalyst was dried at 110°C for 12 h and calcined at 500°C for 5 h [27, 22].

Method of CuO/ZSM-5 Catalyst Synthesis

First of all, Cu precursor dissolved in appropriate ratios in water and pH of the solution controlled by NH_3. In next step, impregnation was done by mixing support with the obtained solution in the previous step. After impregnation, the solution dried at 110°C for 24 h and calcined at 550°C under air flow. In this step, the catalyst is synthesized by the conventional impregnation method. Next, the catalyst shaped cylindrically to be used for performance tests in the reactor.

Experimental Setup

Figure 2 shows a scheme of the experimental system. After studying structural specifications of synthesized catalyst, ethylene to propylene low-pressure pilot was used to evaluate their activity and performance over the process. A pilot was designed and made for the catalytic conversion of ethylene to propylene. In this pilot, liquid and gas were able to be injected concurrently and a precise system of temperature control was considered for micro-reactor and electric oven. Such features as adjustability and flow rate control of gas and liquid flows are provided by the pilot to make diverse detention times of ethylene. For efficiency assessment of synthesized catalysts of ethylene to propylene process, such parameters as catalyst amount and flow rate of input feed were kept 1.2 g and 0.5 cc min^{-1}, respectively. Also, ethylene to propylene reaction was accomplished in a fixed-bed reactor with stainless steel materials, length of 500 mm, the internal diameter of 7 mm in a temperature of 400°C and pressure of 1 atm. The low-nitrogen flow was used for better distribution and prevention of evaporated ethylene backflow. In ethylene to propylene process, the value of output liquid hydrocarbons from micro-reactor was measured in percentage to assess the type of the produced hydrocarbons by Varian gas chromatography (Model CP-3800 made in the US). The used gas chromatography device in the present study had FID indicator and the column used in this device

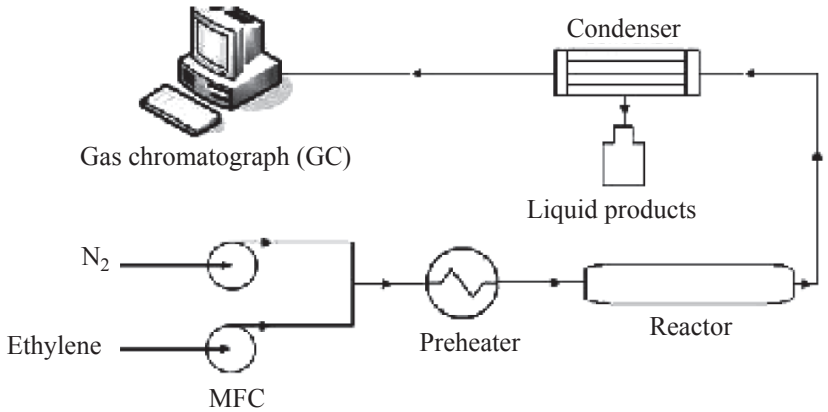

Fig. 2. Experimental system for evaluation of ZSM-5 catalyst synthesis performance for ethylene to propylene conversion.

Table 1. Physicochemical properties of different zeolite samples

Catalyst	Si/AL	SiO_2/Al_2O_3	Crystal size, nm	BET surface area, $m^2\ g^{-1}$	Pore volume, $cm^3\ g^{-1}$
ZSM-5	15	30	17	300	0.39
CuO/ ZSM-5(5%)	12	24	28	280	0.36
CuO/ ZSM-5 (7%)	11	22	30	254	0.33
CuO/ ZSM-5 (9%)	10	20	32	245	0.32
CuO/ ZSM-5 (11%)	9	18	34	230	0.30

was Petrocol DH with a length of 60 m and diameter of 0.25 mm. Helium was used as carrier gas.

RESULTS AND DISCUSSION

Characterization Results

XRD analysis. Figure 3 indicates the spectra associated with XRD analysis for Zeolite ZSM-5. As it can be seen, the spectrum has some prominent peaks associated with Zeolite ZSM-5. The relative crystalline mode of this catalyst was calculated according to a reference, considering prominent peaks angles of 22–25°. The comparison of X-Ray Diffraction data from produced Zeolite sample shows crystalline phase of ZSM-5 in crystal structure. Debye-Scherer equation is used for calculation of mean crystal size of particles (μm) which is defined as follows:

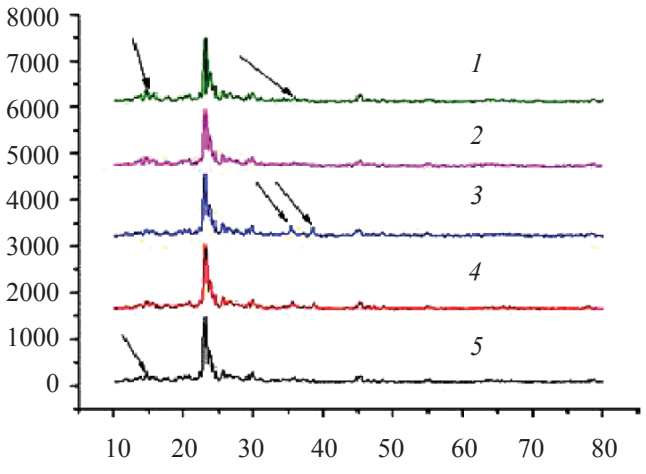

Fig. 3. (Color online) XRD pattern for prepared catalyst. (*1*) CUO/ZSM-5 (11%), (*2*) CUO/ZSM-5 (9%), (*3*) CUO/ZSM-5 (7%), (*4*) CUO/ZSM-5 (5%), (*5*) ZSM-5. The same for Fig. 4.

$$D = K/(\beta \cos \theta). \quad (1)$$

In this formula, λ is the wavelength of X-ray and D is mean size or thickness of the crystal perpendicular to the diffraction plane. K is the constant of the equation and depends on crystalline system and also selection of integral width or Full Width at Half Maximum (FWHM). This constant is about 0.9. β is the angle width or Full Width at Half Maximum (FWHM) and is calculated in radian. θ is the peak angle in degrees. Crystal size for different samples have been calculated using Scherrer equation and been presented in Table 1. After impregnation, crystal size of ZSM-5 zeolite has been increased from 17 nm to 34 nm for zeolite loaded with 5 and 11% CuO, respectively.

FTIR analysis. Spectrum of molecular vibrations is considered as a unique specification and describes features of a molecule. In fundamental and simple terms, infrared spectrum is known as result absorption of electromagnetic radiation in the frequencies which show a relation with vibration of specific sets to chemical bonds from inside the molecule. Therefore, description of IR spectrum encompasses relation and correlation of frequencies for all types of bonds [23]. Vibrational frequencies can be divided into two wide groups: group frequencies and fingerprint frequencies. The former explains group specifications of atoms (e.g. $–CH_3$ and –OH) and helps for characterization and description of a compound. However, the latter describes excellent specifications of specific molecule. Combination of the bonds which are along with both group and fingerprint frequencies is used to determine a specific composition [24]. Figure 4 shows FTIR spectroscopy analysis for Zeolite ZSM-5. In FTIR spectrum, zeolites are seen in two peak categories. The first category is dedicated to internal vibrations of TO_4 (i.e. primary unit of the structure). T means the element inside Zeolite structure

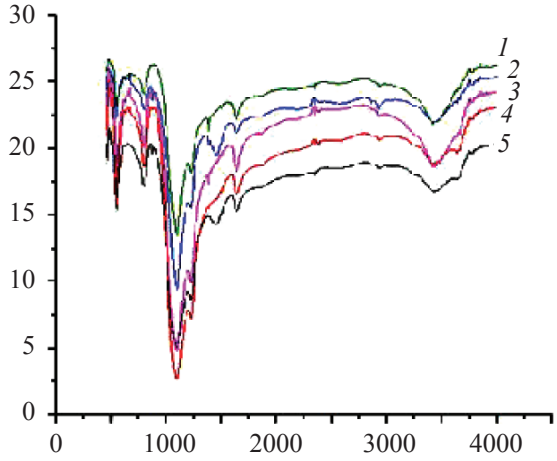

Fig. 4. FTIR analysis pattern results for prepared catalyst.

which is linked to oxygen (e.g. Si and Al). These peaks are typically in the 950–1250 and 420–500 cm^{-1} area which are attributed to T–O and O–T–O stretching vibrations, respectively. The second category contains the vibrations associated with tetrahedral connections. The first observed seen ones frjom the second category are appeared in the 500–600 and 1300–1700 cm^{-1} area. Zooming FTIR spectrum in Fig. 4, we can precisely investigate absorbance compositions around 3400 cm^{-1} which are associated with hydroxide link. As it can be seen from this Fig. 4, this spectrum contains 3 peaks around stretching area of OH group within wave numbers of 3432, 3610, and 3732 cm^{-1}. The observed link in 3732 cm^{-1} is associated with Silanol (Si–OH) group and 3610 cm^{-1} is correlated with acidic zeolite hydroxyls and the link 3432 cm^{-1} is corresponded to the functional group AL–OH.

SEM analysis. Figure 5 shows SEM analysis results for calcined catalyst which were photographed with a zooming of 10. As it can be seen from micro-graph, the sample crystals have a suitable dispersion and regular morphology. These results are in a good agreement with the crystalline size achieved by XRD data. The SEM photographs of calcined and CuO impregnated ZSM-5 catalysts also show that the particles are spherical in shape. Typical SEM images of ZSM-5 and CuO/ZSM-5 are shown in Fig. 5. There was no the significant change in the crystal morphology after CuO loading.

BET analysis. Table 2 present physical and chemical properties of catalyst ZSM-5 and CuO/ ZSM-5 obtained by using BET analysis. Also, BET analysis was conducted to be informed of specific surface area, size and volume of pores. Specific surface area of the catalyst of CuO/ ZSM-5 was decreased from 300 to 200 m^2/g by increasing copper oxide from 0 to 11 wt %. Also, total pores volume was decreased from 0.39 to 0.30 cm^3/g by increasing copper oxide from 0 to 11 wt %, as well. The results show that zeolite ZSM-5 retains its MFI structure by adding up to 11% by weight of copper oxide, and the structure still has acceptable crystallinity. Amin et al. Have claimed that by reducing the size of the crystal, the structure of the network has a greater defect, and this shortage of the network has reduced peak intensity [25–31].

Effect of temperature on rate of ethylene conversion by CuO/ ZSM-5. Figure 6 present effect

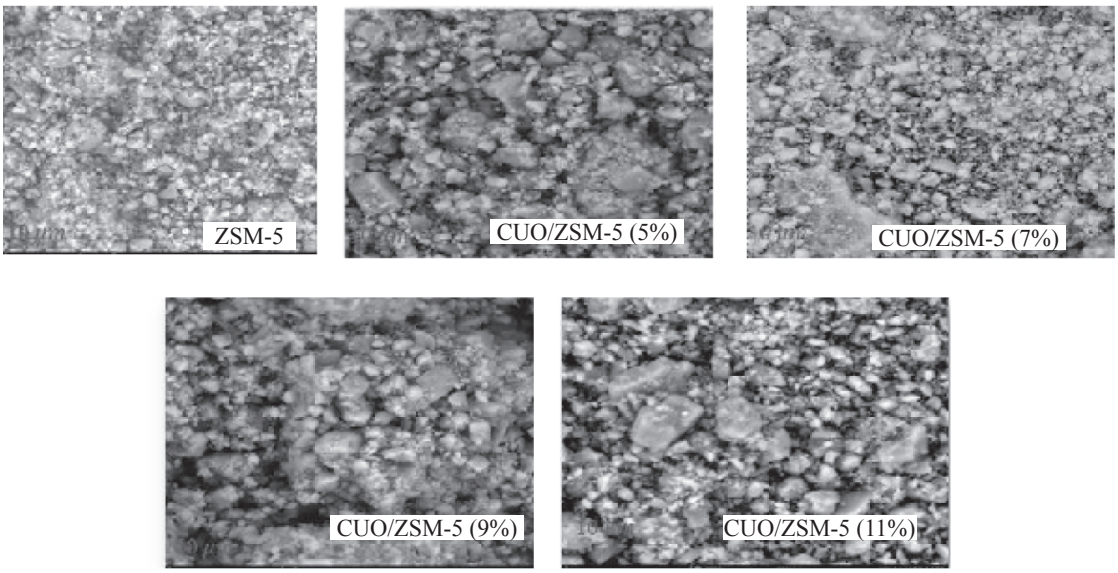

Fig. 5. SEM analysis for prepared catalyst.

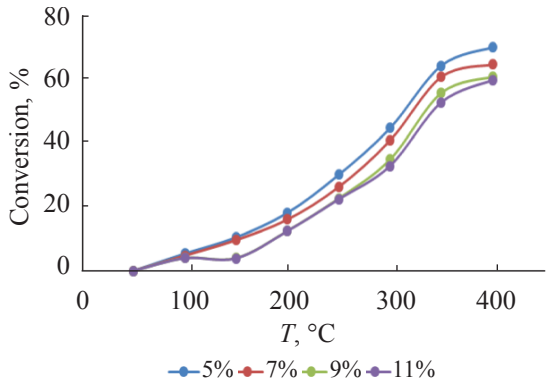

Fig. 6. (Color online) Ethylene conversion rates in terms of temperature using CuO/ZSM-5.

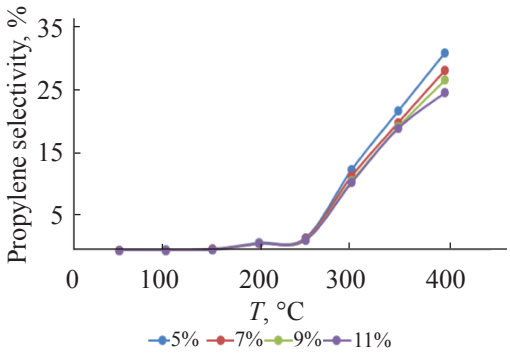

Fig. 7. (Color online) Selectivity of propylene rates in terms of temperature using CuO/ZSM-5.

of temperature on ethylene to propylene conversion rate at diverse temperatures on the ZSM-5 catalysts modified by copper oxide. Figure 6 show conversion rate of ethylene according to temperature using CuO/ZSM-5 catalysts with 5, 7, 9, and 11 wt %. As it can be seen from Fig. 6, ethylene conversion rate increases in higher temperatures and the ascendant trend are seen. Maximum and minimum conversion rates are seen at 400°C and 50°C, respectively. As can be seen in Fig. 6, a catalyst with 5 wt % copper oxide has a better conversion than other percentages.

Effect of temperature on selectivity of propylene with CUO/ ZSM-5 catalyst. Figure 7 presents impact of temperature on the selectivity of propylene on the ZSM-5 catalysts modified by copper oxide. Figure 7 shows diagram of selectivity according to temperature, by using CuO/ZSM-5 catalysts with wt % of 5, 7, 9, and 11. The effect of temperature on the selectivity of propylene on copper oxide modified ZSM-5 catalysts is shown in Fig. 7. As can be seen from Fig. 7, a catalyst with 5 wt % copper oxide has a better selectivity than other percentages.

Table 2. BET results for different synthesized catalysts

Catalyst	BET surface area, $m^2\ g^{-1}$	Pore volume, $cm^3\ g^{-1}$
ZSM-5	300	0.39
CuO (5%) / ZSM-5	265	0.36
CuO (7%) / ZSM-5	254	0.33
CuO (9%) / ZSM-5	204	0.31
CuO (11%) / ZSM-5	200	0.30

CONCLUSIONS

In this article, zeolite ZSM-5 was used as the catalytic base for production of light olefins. Also, the copper oxide was employed to improve the performance of the catalyst. The results of catalytic cracking using the mentioned catalyst showed increased selectivity of light olefin versus thermal cracking at diverse temperatures. The analyses XRD, BET, FTIR, and SEM were conducted on some of the modified samples and the results showed that the catalyst structure was kept intact following adding copper oxide. The results indicated that the selectivity of ethylene and propylene on the catalyst with modified metal of copper oxide would have an ascending trend by increasing the temperature and the maximal selectivity will be obtained at 400°C.

NOMENCLATURE

T: temperature, °C.
id: internal diameter, mm.
F_{A0}: molar flowrate of methanol, cc min^{-1}.
W: weight of catalyst, g.

REFERENCES

1. Noyen, J.V., Wilde, A.D., Schroeven, M., et al., *Int. J. Appl. Ceramic Technology*, 2012, vol. 9, pp. 902–910.
2. Narula, C.K., Daw, C.S., Hoard, J.W., et al., *Int. J. Appl. Ceramic Technology*, 2005, vol. 2, pp. 452–466.
3. Singh, R.N., *Int. J. Appl. Ceramic Technology*, 2007, vol. 4, pp. 134–144.
4. Aghaei, E. and Haghighi, M., *Microporous Mesoporous Mater.*, 2014, vol. 196, pp. 179–190.
5. Amereh, M., Haghighi, M., Estifaee, P., *Arabian J.*

Chem., (In Press).

6. Estifaee, P., Haghighi, M., Babaluo, A., et al., *J. Power Sources*, 2015, vol. 257, pp. 364–373.
7. Fathi, S., Sohrabi, M., and Falamaki, C., *Fuel*, 2014, vol. 116, pp. 529–537.
8. Rahemi, N., Haghighi, M., Babaluo, A., et al., *Int. J. Energy Res.,* 2014, vol. 38, pp. 765–779.
9. Brzozowski, R., *Applied Catalysis A: General*, 2004, vol. 27, pp. 215–218.
10. Gauthier, C., Chiche, B., Finiels, A., et al., *J. Molecular Catalysis*, 1989, vol. 50, pp. 219–229.
11. Walendziewski, J. and Trawczyn, J., *Ind. & Eng. Chem. Res.,* 1996, vol. 35, pp. 3356–3361.
12. Hathaway, P.E. and Davis, M.E., *J. Catalysis*, 1989, vol. 119, pp. 497–507.
13. Sugi, Y., *J. Chinese Chemical Soc.*, 2010, vol. 57, pp. 1–13.
14. Bouvier, C., Buijs, W., Gascon, J., et al., *J. Catalysis,* 2010, vol. 270, pp. 60–66.
15. Kamalakar, G., Ramakrishna, M., Kulkarni, S.J., et al., *Microporous & Mesoporous Materials*, 2000, 38, pp. 135–142.
16. Kamalakar, G., Prasad, M.R., Kulkarni, S.J., et al., *Microporous & Mesoporous Materials*, 2002, vol. 52, pp. 151–158.
17. Addiego, W.P., Brundage, K.R., Glose, C.R., in *Corning Incorporated,* 2005, New York: Corning, 244, 689 B2.
18. Campanati, M., Fornasari, G., and Vaccari, A., *Catalysis Today*, 2003, vol. 77, pp. 299–314.
19. Nelson, H.C., Lussier, R.J., Still, M.E., *Applied Catalysis*, 1983, vol. 7, pp. 113–121.
20. Bouvier, C., Reumkens, N., Buijs, W., *J. Chromatography, A,* 2009, vol. 1216, pp. 6410–6416.
21. Wang, Y., Xu, L., Yu, Z., et al., *Catalysis Communications,* 2008, vol. 9, pp. 1982–1986.
22. Zhang, K.F., *J. Power Sources,* 2006, vol. 162, pp. 1077–1081.
23. Spahr, M.E., *J. Electrochem. Soc.,* 1999, vol. 46, pp. 2780–2783.
24. Cañzares, P., Lucas, A.D., Dorado, F., et al., *Appl. Catal. A: Gen.*, 1998, p. 169.
25. Donk, S.V., Janssen, A.H., Bitter, J.H., et al., *Catal. Rev*., 2003, p. 45.
26. Leach, E. and Bruce, E., *Industrial Catalysis*, 1983, vol. 1, New York: Academic Press, Inc.
27. Jacobs, G. and Davis, B.H., In *Catalysis*, Spivey, J.J and Dooley, K.M., Eds., Cambridge, The Royal Society of Chemistry, 2007, p. 20.
28. Kianfar, E., Salimi, M., Pirouzfar, V., and Koohestani, B., *Int. J. Appl. Ceramic Technology*, 2017, vol. 15, no. 3, pp. 734–741.
29. Kianfar, E., Salimi, M., Pirouzfar, V., and Koohestani, B., *Int. J. Chem. React. Eng., B,* vol. 16, no. 7, pp. 1–7.
30. Kianfar, E., Salimi, M., Hajimirzaee, S., and Koohestani, B., *Int. J. Chem. React. Eng.*, 2018, https://doi.org/10.1515/ijcre-2018-0127.
31. Kianfara, E., *Russ. J. Appl. Chem.*, 2018, vol. 91, no. 10, pp. 1710–1720.